Ann. Solid Struct. Mech. (2012) 4:15–23
DOI 10.1007/s12356-012-0029-9

ORIGINAL ARTICLE

Frequency-locking in nonlinear forced oscillators near 3:1 and 4:1 resonances

Mohamed Belhaq · Abdelhak Fahsi

Received: 9 March 2011 / Accepted: 30 October 2012 / Published online: 16 November 2012

Abstract In this paper, frequency-locking phenomenon in self-excited nonlinear oscillators subjected to harmonic excitation is investigated near the 3:1 and 4:1 subharmonic resonances. Analytical treatment based on perturbation techniques is performed to study the quasiperiodic modulation domain and the frequency-locking area in the vicinity of these resonances. It is shown that this analytical method, based on a double averaging procedure, is efficient to capture the modulation domain of the quasiperiodic response as well as the threshold of synchronization area near the considered subharmonic resonances.

Keywords Frequency locking · Self-excitation · Subharmonic resonance · Quasiperiodic modulation · Perturbation analysis

1 Introduction

In self-excited nonlinear oscillators subjected to harmonic forcing, frequency-locking behavior can occur near resonances. This phenomenon results from synchronization near the resonances between the frequency of the periodic forcing of the system and the frequency of the self excitation leading to frequency-locked motions for which the response of the system follows the forcing frequency. Away from the resonances the response is quasiperiodic. Usually, the transition between quasiperiodic and synchronized motions can take place at two different specific frequencies when the forcing frequency is swept backward and forward producing hysteresis and abrupt jumps in the system response. These jumps phenomena are considered as serious physical problems that may cause the failure of systems and therefore analytical approximation of their location is of great importance from application view point. The presence of hysteresis near a resonance is associated with the coexistence of two distinct stable states (periodic and quasiperiodic) and hence, jump occurs between these two states. In this context, the control of hysteresis is an importance issue to realize a high functionality of systems and to improve their specific performance. For instance, the attenuation of hysteresis in micro-electro-mechanical systems resonators was performed by acting on the quality factor which is related to the damping [1] and the suppression of hysteresis in a forced van der Pol-Duffing oscillator was reported near resonances [2, 3].

The purpose of the present paper is to investigate analytically the frequency-locking area near the subharmonic resonance of order 3 and 4. For the 3:1 resonance, we consider a van der Pol-Duffing oscillator submitted to external harmonic excitation, whereas a van der Pol–Mathieu oscillator with a quadratic nonlinearity is considered for studying the frequency-locking near the 4:1 resonance. A perturbation method [4, 5] is applied in a first step to derive an autonomous slow flow system and analysis of equilibria of this slow flow provides analytical approximations of the amplitude-frequency response. A second perturbation method is performed in a second step on the slow flow to approximate quasiperiodic solution and its modulation domain. Numerical simulation is performed to compare with the analytical finding for validation. It is worthy noticing that the first part of the 3:1 subharmonic

M. Belhaq (✉)
University Hassan II-Casablanca, Casablanca, Morocco
e-mail: mbelhaq@yahoo.fr

A. Fahsi
FSTM, University Hassan II-Mohammadia,
Mohammadia, Morocco
e-mail: afahsi2002@yahoo.fr

resonance case has been reported in previous works [6, 7] and presented here for convenience. Therefore, the present paper can be considered as a logical continuity of these previous works.

2 Frequency-locking in the 3:1 subharmonic resonance

To study the frequency-locking (or entrainment) near the 3:1 subharmonic resonance, the following forced van der Pol-Duffing oscillator given in the dimensionless form is considered

$$\ddot{x} + \omega_0^2 x - \varepsilon(\alpha - \beta x^2)\dot{x} - \varepsilon\gamma x^3 = h\cos\omega t \tag{1}$$

where ω_0 is the natural frequency, α, β are the damping coefficients, γ is the nonlinear component and h, ω are the amplitude and the frequency of the external excitation, respectively, and ε is a small parameter introduced to indicate that α, β and γ are small. The purpose is to approximate the amplitude-frequency response of the 3:1 resonance, the quasiperiodic modulation domain and the locations of the frequency-locked response.

2.1 Amplitude-frequency response

To approximate the the amplitude-frequency response near the 3:1 resonance, we express the 3:1 resonance condition by introducing a detuning parameter σ according to

$$\omega_0^2 = \left(\frac{\omega}{3}\right)^2 + \varepsilon\sigma \tag{2}$$

and we use the method of multiple scales [5] on Eq. (1) which can be rearranged in the form

$$\ddot{x} + \left(\frac{\omega}{3}\right)^2 x = h\cos\omega t + \varepsilon\{-\sigma x + (\alpha - \beta x^2)\dot{x} + \gamma x^3\} \tag{3}$$

We seek a two-scale expansion of the solution in the form

$$x(t) = x_0(T_0, T_1) + \varepsilon x_1(T_0, T_1) + O(\varepsilon^2) \tag{4}$$

where x_0, x_1 are, respectively, the zero and the first order approximations of the solution and $T_i = \varepsilon^i t$ $(i = 0, 1, 2)$ are the different time scales. In terms of the variables T_i, the time derivatives become $\frac{d}{dt} = D_0 + \varepsilon D_1 + \varepsilon^2 D_2 + O(\varepsilon^3)$ and $\frac{d^2}{dt^2} = D_0^2 + 2\varepsilon D_0 D_1 + \varepsilon^2 D_1^2 + 2\varepsilon^2 D_0 D_2 + O(\varepsilon^3)$, where $D_i^j = \frac{\partial^j}{\partial T_i^j}$. Substituting (4) into (3) and equating coefficients of the same power of ε, we obtain the following set of linear partial differential equations

$$D_0^2 x_0(T_0, T_1) + \left(\frac{\omega}{3}\right)^2 x_0(T_0, T_1) = h\cos\omega T_0 \tag{5}$$

$$D_0^2 x_1(T_0, T_1) + \left(\frac{\omega}{3}\right)^2 x_1(T_0, T_1) = -2D_0 D_1 x_0 - \sigma x_0 + (\alpha - \beta x_0^2) D_0 x_0 + \gamma x_0^3. \tag{6}$$

The solution to the first order is given by

$$x_0(T_0, T_1) = r(T_1)\cos\left(\frac{\omega}{3}T_0 + \theta(T_1)\right) + F\cos\omega T_0 \tag{7}$$

where r and θ are, respectively, the amplitude and the phase of the response and $F = -\frac{9h}{8\omega^2}$. Substituting (7) into (6), removing secular terms and using the expressions $\frac{dr}{dt} = \varepsilon D_1 r + O(\varepsilon^2)$ and $\frac{d\theta}{dt} = \varepsilon D_1\theta + O(\varepsilon^2)$, we obtain the slow flow modulation equations of amplitude and phase

$$\begin{aligned} \frac{dr}{dt} &= Ar - Br^3 - (H_1\sin 3\theta + H_2\cos 3\theta)r^2, \\ \frac{d\theta}{dt} &= S - Cr^2 - (H_1\cos 3\theta - H_2\sin 3\theta)r \end{aligned} \tag{8}$$

where $A = \frac{\alpha}{2} - \frac{\beta F^2}{4}$, $B = \frac{\beta}{8}$, $C = \frac{9\gamma}{8\omega}$, $S = \frac{3\sigma}{2\omega} - \frac{9\gamma F^2}{4\omega}$, $H_1 = \frac{9\gamma F}{8\omega}$ and $H_2 = \frac{\beta F}{8}$. Equilibria of the slow flow (8), corresponding to periodic solutions of Eq. (1), are determined by setting $\frac{dr}{dt} = \frac{d\theta}{dt} = 0$. This leads to the amplitude-frequency response equation

$$A_2 r^4 + A_1 r^2 + A_0 = 0 \tag{9}$$

where $A_2 = B^2 + C^2$, $A_1 = -(2AB + 2SC + H_1^2 + H_2^2)$ and $A_0 = A^2 + S^2$.

Figure 1 shows the variation of the amplitude-frequency response curve, as given by (9), for the given parameters $\alpha = 0.01$, $\beta = 0.05$, $\gamma = 0.1$ and $h = 1$. The solid line denotes the stable branch and the dashed line denotes the unstable one. The stability analysis has been done using the Jacobian of the slow flow system (8). Results from numerical simulation (circles) using Runge-Kutta method are also plotted for validation.

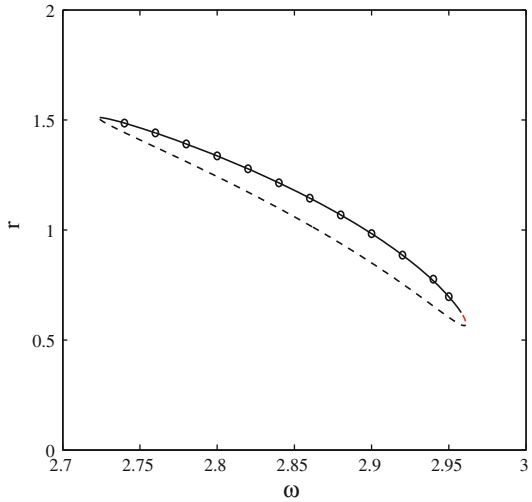

Fig. 1 Amplitude-frequency response curve near 3:1 resonance. *Solid line* for stable, *dashed line* for unstable and *circles* for numerical simulation, $\alpha = 0.01$, $\beta = 0.05$, $\gamma = 0.1$, $h = 1$

2.2 Quasiperiodic modulation domain

To approximate quasiperiodic solutions of (1), corresponding to periodic solutions of the slow flow (8), we perform a second perturbation analysis on the following slow flow cartesian system equivalent to the polar form (8)

$$\begin{aligned}\frac{du}{dt} &= Sv + \mu\{Au - (Bu + Cv)(u^2 + v^2) \\ &\quad + 2H_1uv - H_2(u^2 - v^2)\}, \\ \frac{dv}{dt} &= -Su + \mu\{Av - (Bv - Cu)(u^2 + v^2) \\ &\quad + H_1(u^2 - v^2) + 2H_2uv\}\end{aligned} \tag{10}$$

where $u = r\cos\theta$ and $v = -r\sin\theta$. The small parameter μ introduced in the equations specifies the scaling of the coefficients that appear therein. Notice that this double perturbation procedure has been successfully applied in previous works to capture the dynamic in quasiperiodic Mathieu equations [8, 9, 10, 11, 12]. We rewrite (10) in the form

$$\begin{aligned}\frac{du}{dt} &= Sv + \mu f(u, v), \\ \frac{dv}{dt} &= -Su + \mu g(u, v)\end{aligned} \tag{11}$$

where $f(u, v)$ and $g(u, v)$ are given in (10).

We use the multiple scales method by expanding solutions of (10) or (11) as

$$\begin{aligned}u(t) &= u_0(T_0, T_1, T_2) + \mu u_1(T_0, T_1, T_2) \\ &\quad + \mu^2 u_2(T_0, T_1, T_2) + O(\mu^3), \\ v(t) &= v_0(T_0, T_1, T_2) + \mu v_1(T_0, T_1, T_2) \\ &\quad + \mu^2 v_2(T_0, T_1, T_2) + O(\mu^3)\end{aligned} \tag{12}$$

where $T_i = \mu^i t$. Substituting (12) into (11) and collecting terms, we get

- Order μ^0:

$$\begin{cases} D_0^2 u_0 + S^2 u_0 = 0, \\ Sv_0 = D_0 u_0 \end{cases} \tag{13}$$

- Order μ^1:

$$\begin{cases} D_0^2 u_1 + S^2 u_1 = -2D_0D_1u_0 + D_0(f(u_0, v_0)) + Sg(u_0, v_0), \\ Sv_1 = D_0u_1 + D_1u_0 - f(u_0, v_0) \end{cases} \tag{14}$$

- Order μ^2:

$$\begin{cases} D_0^2 u_2 + S^2 u_2 = -2D_0D_2u_0 - D_0D_1u_1 - SD_1v_1 \\ \quad + D_0\left(u_1\dfrac{\partial f}{\partial u}(u_0, v_0) + v_1\dfrac{\partial f}{\partial v}(u_0, v_0)\right) \\ \quad + S\left(u_1\dfrac{\partial g}{\partial u}(u_0, v_0) + v_1\dfrac{\partial g}{\partial v}(u_0, v_0)\right), \\ Sv_2 = D_0u_2 + D_1u_1 + D_2u_0 \\ \quad - \left(u_1\dfrac{\partial f}{\partial u}(u_0, v_0) + v_1\dfrac{\partial f}{\partial v}(u_0, v_0)\right) \end{cases} \tag{15}$$

where $D_i^j = \frac{\partial^j}{\partial T_i^j}$. A solution to the first order is given by

$$\begin{aligned}u_0(T_0, T_1) &= R(T_1)\cos(ST_0 + \varphi(T_1)), \\ v_0(T_0, T_1) &= -R(T_1)\sin(ST_0 + \varphi(T_1))\end{aligned} \tag{16}$$

Substituting (16) into (14), removing secular terms and using the expressions $\frac{dR}{dt} = \mu D_1 R + O(\mu^2)$ and $\frac{d\varphi}{dt} = \mu D_1\varphi + O(\mu^2)$, we obtain the following *slow slow* flow system on R and φ

$$\begin{aligned}\frac{dR}{dt} &= AR - BR^3, \\ \frac{d\varphi}{dt} &= -CR^2\end{aligned} \tag{17}$$

Then, the first-order approximate periodic solution of the slow flow (11) is given by

$$\begin{aligned}u(t) &= R\cos\nu t, \\ v(t) &= -R\sin\nu t\end{aligned} \tag{18}$$

where the amplitude R and the frequency ν are obtained by setting $\frac{dR}{dt} = 0$ and given, respectively, by

$$R = \sqrt{\frac{A}{B}} \tag{19}$$

$$\nu = S - CR^2 \tag{20}$$

Using (18), the modulated amplitude of quasiperiodic solution of Eq. (1) is approximated by

$$r(t) = \sqrt{u^2(t) + v^2(t)} = R \tag{21}$$

This indicates that the quasiperiodic modulation area is reduced, at this first-order approximation, to the unique curve given by

$$r_{min} = r_{max} = R \tag{22}$$

where r_{min} and r_{max} designate the maximum and the minimum of the amplitude modulation, respectively.

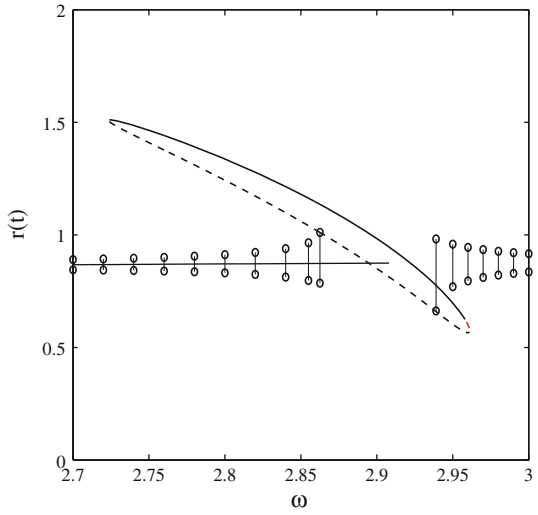

Fig. 2 Amplitude-frequency response curve and modulation amplitude of slow flow limit cycle. Numeric: *double circles*, analytic to the first order: *horizontal line*. Values of parameters are fixed as in Fig. 1

In Fig. 2 the amplitude-frequency response curve as well as the quasiperiodic modulation domain obtained numerically (double circles connected with a vertical line) are shown. The horizontal line lying in the middle of circles corresponds to the first-order approximation of the quasiperiodic modulation domain as given by Eq. (22). Notice that the first-order approximation fails to capture the quasiperiodic modulation domain (double circles).

At the second-order approximation, a particular solution of system (14) is given by

$$\begin{aligned} u_1(T_0,T_1,T_2) &= \frac{R^2(T_1,T_2)}{3S}(H_1\cos(2ST_0+2\varphi(T_1,T_2)) \\ &\quad - H_2\sin(2ST_0+2\varphi(T_1,T_2))), \\ v_1(T_0,T_1,T_2) &= \frac{R^2(T_1,T_2)}{3S}(H_1\sin(2ST_0+2\varphi(T_1,T_2)) \\ &\quad + H_2\cos(2ST_0+2\varphi(T_1,T_2))) \end{aligned} \tag{23}$$

Substituting (16), (19) and (23) into (15) and removing secular terms gives the following partial differential equations on R and φ

$$\begin{aligned} &D_2R = 0, \\ &D_2\varphi = -\frac{2R^2}{3S}(H_1^2+H_2^2) \end{aligned} \tag{24}$$

Then, the second-order approximate periodic solution of the slow flow (11) is given now by

$$\begin{aligned} u(t) &= R\cos vt + \frac{R^2}{3S}(H_1\cos(2vt) - H_2\sin(2vt)), \\ v(t) &= -R\sin vt + \frac{R^2}{3S}(H_1\sin(2vt) + H_2\cos(2vt)) \end{aligned} \tag{25}$$

where the amplitude R and the frequency v are obtained by setting $\frac{dR}{dt} = D_1R + D_2R = 0$ and given, respectively, by

$$R = \sqrt{\frac{A}{B}} \tag{26}$$

$$v = S - \left(C + \frac{2R^2}{3S}\left(H_1^2+H_2^2\right)\right)R^2 \tag{27}$$

The modulated amplitude of quasiperiodic solution is now approximated by

$$r(t) = \sqrt{R^2 + \frac{R^4}{9S^2}(H_1^2+H_2^2) + \frac{2R^3}{3S}(H_1\cos(3vt) - H_2\sin(3vt))} \tag{28}$$

and the envelope of this modulation is delimited by r_{min} and r_{max} given by

$$r_{min} = \sqrt{R^2 + \frac{R^4}{9S^2}(H_1^2+H_2^2) - \frac{2R^3}{3S}\sqrt{H_1^2+H_2^2}} \tag{29}$$

$$r_{max} = \sqrt{R^2 + \frac{R^4}{9S^2}(H_1^2+H_2^2) + \frac{2R^3}{3S}\sqrt{H_1^2+H_2^2}} \tag{30}$$

In Fig. 3 we show the modulated amplitude of the quasiperiodic solution (solid lines), as given by Eqs. (29), (30). The comparison between this analytical prediction and the numerical simulations (circles) indicates that the second-order analytical approximation can capture the quasiperiodic modulation domain. It can be seen from this figure that outside the synchronization area quasiperiodic behavior takes place. When approaching the synchronization area, the upper limit of the modulation amplitude collides with the unstable branch producing a frequency-locking.

Figure 4 illustrates examples of phase portraits of the slow flow (10) for some values of ω picked from Fig. 3.

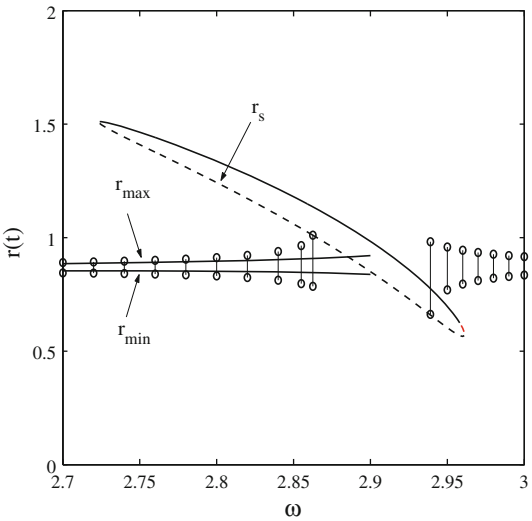

Fig. 3 Modulation amplitude of slow flow limit cycle. Numerical simulation: *double circles*, analytical approximation to the second order: *double lines*; r_s: saddles amplitude. Values of parameters are fixed as in Fig. 1

For small values of ω, a slow flow limit cycle born by Hopf bifurcation exists and attracts all initial conditions. The related phase portraits are shown in subfigure (a) for $\omega = 2.72$. The subfigure (b) for $\omega = 2.80$ indicates the coexistence of a stable periodic orbit (stable equilibrium born by saddle-node bifurcation) and quasiperiodic (stable limit cycle) responses. As the forcing frequency varies, the stable slow flow limit cycle approaches the saddles and disappears via a heteroclinic bifurcation. The corresponding phase portrait is shown in subfigure (c) for the value $\omega = 2.86256$. This mechanism gives rise to frequency-locking, in which the response of the system follows the 3:1 subharmonic frequency (see subfigure (d) for $\omega = 2.90$). We point out that in this study, we have approximated the analytically quasiperiodic modulated domain in the case where the limit cycle disappears leaving the cycles located outside the heteroclinic connection, as shown in Fig. 4b,c. The other case of heteroclinic bifurcation leaving the cycles inside the connection is not considered here. The phase portraits corresponding to this bifurcation are illustrated in Fig. 4e,f.

3 Frequency-locking in the 4:1 subharmonic resonance

To investigate the frequency-locking near the 4:1 resonance, we consider a van der Pol–Mathieu oscillator with a quadratic nonlinearity given in the dimensionless form as

$$\ddot{x} + \omega_0^2(1 + \varepsilon h \cos \omega t)x - (\varepsilon^2\alpha - \varepsilon\beta x)\dot{x} - \varepsilon c x^2 = 0 \qquad (31)$$

where ω_0 is the natural frequency, α, β are the damping coefficients, c is the quadratic component, h, ω are, respectively, the amplitude and the frequency of the parametric excitation, and ε is introduced for scaling the parameters. It is worth noticing that while the dynamic and the local bifurcations of Eq. (31) near the 4:1 resonances

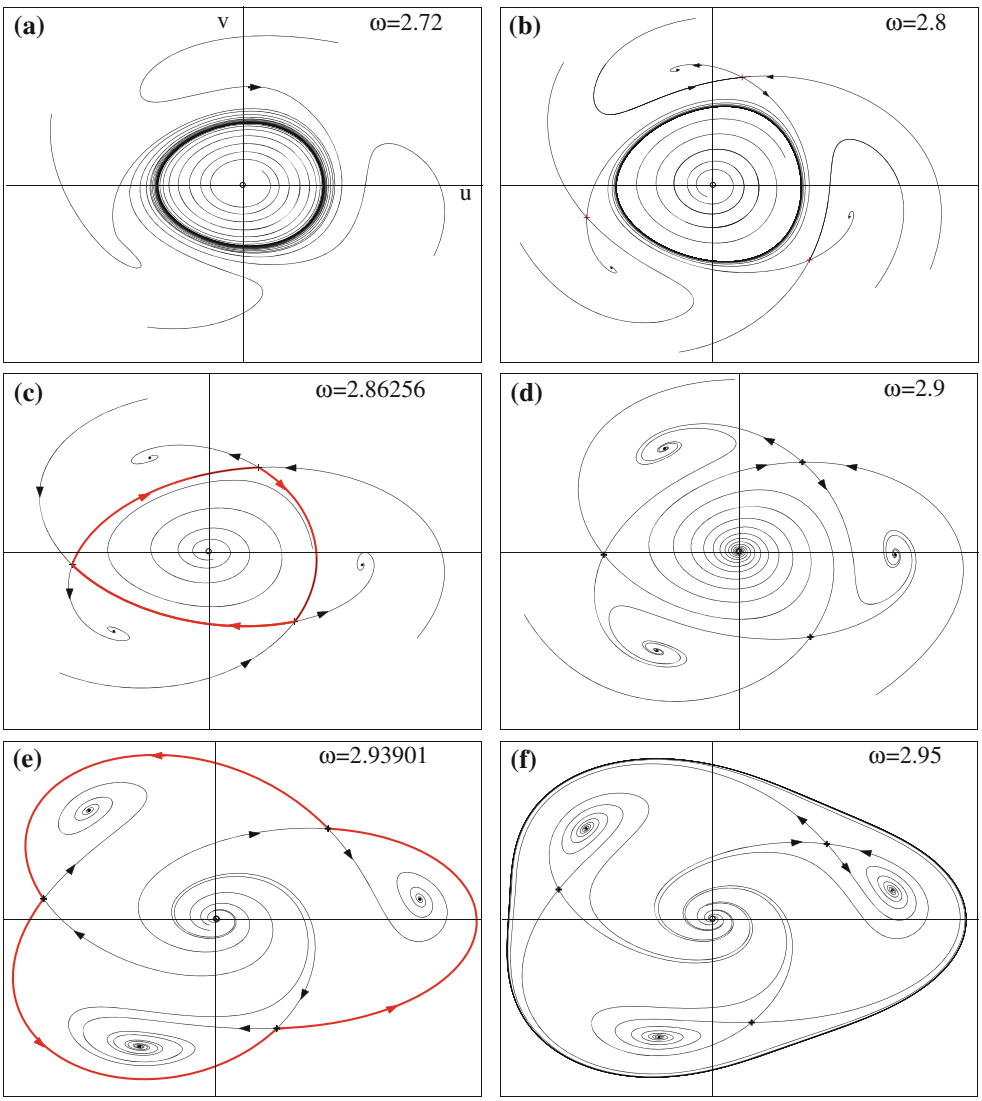

Fig. 4 Examples of phase portraits of the slow flow at different frequencies picked from Fig. 3. Values of parameters are fixed as in Fig. 1

has been extensively studied [13, 14], the investigation of the global bifurcations corresponding to the frequency-locking threshold is still unexplored from analytical view point.

Our purpose here is to approximate the amplitude-frequency response near the 4:1 resonance and the modulation domain of the quasiperiodic response of Eq. (31) as well.

3.1 Amplitude-frequency response

We impose the 4:1 resonance condition by introducing a detuning parameter σ according to

$$\omega_0^2 = \left(\frac{\omega}{4}\right)^2 + \varepsilon^2\sigma \tag{32}$$

We use the method of Bogoliubov-Mitropolsky [4] on Eq. (31) which can be rearranged in the form

$$\begin{aligned}\ddot{x} + \left(\frac{\omega}{4}\right)^2 x = {} & \varepsilon\{cx^2 - \beta x\dot{x} - h\left(\frac{\omega}{4}\right)^2 x\cos\omega t\} \\ & + \varepsilon^2\{-\sigma x + \alpha\dot{x}\}\end{aligned} \tag{33}$$

Following previous works [15], the expressions of the 4:1 subharmonic solution up to the third order are given by

$$\begin{aligned}x(t) = {} & r\cos\left(\frac{\omega}{4}t+\theta\right) + \frac{8cr^2}{\omega^2} - \frac{8cr^2}{3\omega^2}\cos\left(\frac{\omega}{2}t+2\theta\right) \\ & - \frac{2\beta r^2}{3\omega}\sin\left(\frac{\omega}{2}t+2\theta\right) + \frac{hr}{48}\cos\left(\frac{5\omega}{4}t+\theta\right) \\ & + \frac{hr}{16}\cos\left(\frac{3\omega}{4}t-\theta\right) \\ & + \left(\frac{16c^2}{3\omega^4} - \frac{\beta^2}{2\omega^2}\right)r^3\cos\left(\frac{3\omega}{4}t+3\theta\right) \\ & + \frac{10\beta cr^3}{3\omega^3}\sin\left(\frac{3\omega}{4}t+3\theta\right) + \frac{4hcr^2}{9\omega^2}\cos(\omega t) \\ & - \frac{2h\beta r^2}{45\omega}\sin(\omega t) - \frac{7hcr^2}{9\omega^2}\cos\left(\frac{\omega}{2}t-2\theta\right) \\ & + \frac{h\beta r^2}{36\omega}\sin\left(\frac{\omega}{2}t-2\theta\right) - \frac{hcr^2}{21\omega^2}\cos\left(\frac{3\omega}{2}t+2\theta\right) \\ & - \frac{h\beta r^2}{60\omega}\sin\left(\frac{3\omega}{2}t+2\theta\right) + \frac{h^2 r}{1536}\cos\left(\frac{7\omega}{4}t-\theta\right) \\ & + \frac{h^2 r}{7680}\cos\left(\frac{9\omega}{4}t+\theta\right)\end{aligned} \tag{34}$$

where r and θ are, respectively, the amplitude and the phase of the response which are solutions of the following slow flow modulation system

$$\begin{aligned}\frac{dr}{dt} &= Ar - Br^3 - (H_1\sin 4\theta + H_2\cos 4\theta)r^3 \\ \frac{d\theta}{dt} &= S - Cr^2 - (H_1\cos 4\theta - H_2\sin 4\theta)r^2\end{aligned} \tag{35}$$

Here $A = \frac{\alpha}{2}$, $B = \frac{16\beta c}{8\omega^2}$, $C = \frac{80c^2}{3\omega^3} + \frac{\beta 2}{6\omega}$, $S = \frac{2\sigma}{\omega} + \frac{h^2\omega}{192}$, $H_1 = -\frac{20hc^2}{9\omega^3} + \frac{h\beta^2}{72\omega}$ and $H_2 = \frac{h\beta c}{9\omega^2}$. The detailed calculation to obtain the expression of the solution (34) is given in [15].

Equilibria of this slow flow correspond to periodic solutions of Eq. (31) which are determined by setting $\frac{dr}{dt} = \frac{d\theta}{dt} = 0$. This leads to the amplitude-frequency response equation

$$A_2 r^4 + A_1 r^2 + A_0 = 0 \tag{36}$$

where $A_2 = B^2 + C^2 - H_1^2 - H_2^2$, $A_1 = -2(AB + SC)$ and $A_0 = A^2 + S^2$.

Figure 5 illustrates the variation of the amplitude-frequency response curve, as given by (36), for the given parameters α, $= 0.01$, $\beta = 0.2$, $c = 1$ and $h = 0.2$. The solid line denotes the stable branch and the dashed line denotes the unstable one. The validity of the analytical approximations (34) is tested by performing numerical simulations on Eq. (31) using the fourth–order Runge–Kutta method as shown in Fig. 6. This figure shows the result in the phase portrait of (31) for the parameter values given above. The solid line is obtained from the analytical expression (34), while the dotted line is obtained by direct numerical simulations of (31).

3.2 Quasiperiodic modulation domain

Next we explore the periodic motions of the slow flow (35) corresponding to quasiperiodic solution of the original system (31). Such a periodic solution can be approximated by performing a perturbation analysis on the slow flow (35) or on the corresponding Cartesian one

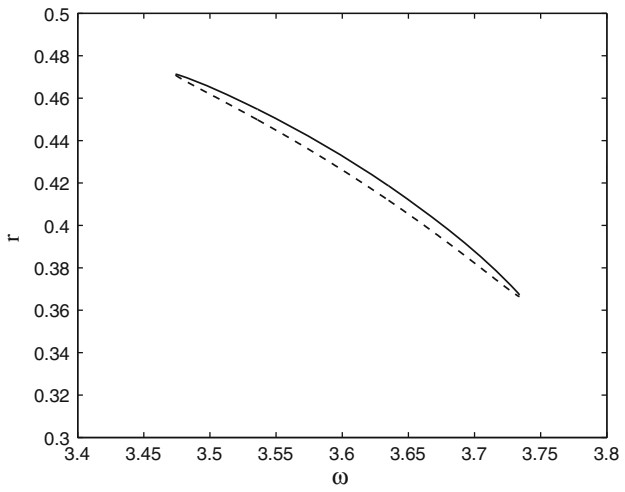

Fig. 5 Amplitude−frequency response curve near the 4:1 resonance. *Solid line* for stable and *dashed line* for unstable, $\alpha = 0.01$, $\beta = 0.2$, $c = 1$, $h = 0.2$

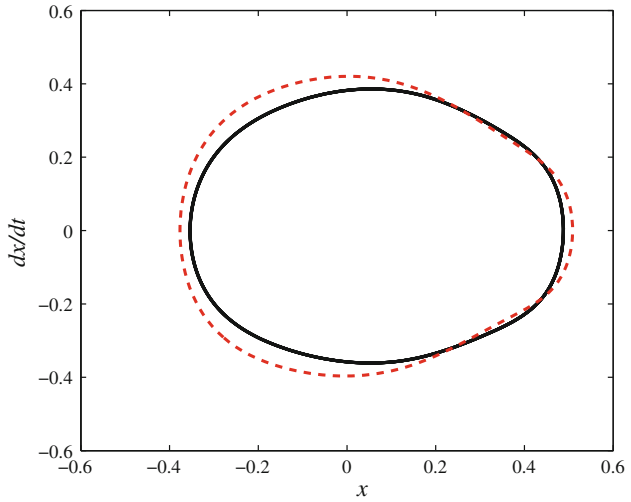

Fig. 6 Comparison between the analytical approximation, (34), (*solid line*) and the numerical integration of (31) (*dotted line*). Values of parameters are fixed as in Fig. 5

$$\begin{aligned}\frac{du}{dt} &= Sv + \mu(Au - (Bu + Cv)(u^2 + v^2) - H_1 v(v^2 - 3u^2) \\ &\quad - H_2 u(u^2 - 3v^2)) \\ \frac{dv}{dt} &= -Su + \mu(Av - (Bv - Cu)(u^2 + v^2) + H_1 u(u^2 - 3v^2) \\ &\quad - H_2 v(v^2 - 3u^2))\end{aligned} \tag{37}$$

where $u = r\cos\theta$ and $v = -r\sin\theta$. The small parameter μ introduced in the equations specify the scaling of the coefficients that appear therein. The system (37) can be written in the compacted form

$$\begin{cases} \dfrac{du}{dt} = Sv + \mu f(u, v), \\ \dfrac{dv}{dt} = -Su + \mu g(u, v) \end{cases} \tag{38}$$

where $f(u, v)$ and $g(u, v)$ are given explicitly in (37). Using the multiple scales method, the solutions of (38) are expanded as

$$\begin{aligned} u(t) &= u_0(T_0, T_1, T_2) + \mu u_1(T_0, T_1, T_2) \\ &\quad + \mu^2 u_2(T_0, T_1, T_2) + O(\mu^3), \\ v(t) &= v_0(T_0, T_1, T_2) + \mu v_1(T_0, T_1, T_2) \\ &\quad + \mu^2 v_2(T_0, T_1, T_2) + O(\mu^3) \end{aligned} \tag{39}$$

where $T_i = \mu^i t$. Substituting (39) into (38) and collecting terms, we get

- Order μ^0:

$$\begin{cases} D_0^2 u_0 + S^2 u_0 = 0, \\ Sv_0 = D_0 u_0 \end{cases} \tag{40}$$

- Order μ^1:

$$\begin{cases} D_0^2 u_1 + S^2 u_1 = -2D_0 D_1 u_0 + D_0(f(u_0, v_0)) + Sg(u_0, v_0), \\ Sv_1 = D_0 u_1 + D_1 u_0 - f(u_0, v_0) \end{cases} \tag{41}$$

- Order μ^2:

$$\begin{cases} D_0^2 u_2 + S^2 u_2 = -2D_0 D_2 u_0 - D_0 D_1 u_1 - SD_1 v_1 \\ \quad + D_0\left(u_1 \dfrac{\partial f}{\partial u}(u_0, v_0) + v_1 \dfrac{\partial f}{\partial v}(u_0, v_0)\right) \\ \quad + S\left(u_1 \dfrac{\partial g}{\partial u}(u_0, v_0) + v_1 \dfrac{\partial g}{\partial v}(u_0, v_0)\right), \\ Sv_2 = D_0 u_2 + D_1 u_1 + D_2 u_0 \\ \quad - \left(u_1 \dfrac{\partial f}{\partial u}(u_0, v_0) + v_1 \dfrac{\partial f}{\partial v}(u_0, v_0)\right) \end{cases} \tag{42}$$

where $D_i^j = \frac{\partial^j}{\partial T_i^j}$. A solution to the first order of system (40) is given by

$$\begin{aligned} u_0(T_0, T_1) &= R(T_1)\cos(ST_0 + \varphi(T_1)), \\ v_0(T_0, T_1) &= -R(T_1)\sin(ST_0 + \varphi(T_1)) \end{aligned} \tag{43}$$

Substituting (43) into (41), removing secular terms and using the expressions $\frac{dR}{dt} = \mu D_1 R + O(\mu^2)$ and $\frac{d\varphi}{dt} = \mu D_1 \varphi + O(\mu^2)$, we obtain a *slow slow* flow system on R and φ similar to (17).

At the second-order approximation, a particular solution of system (41) is given by

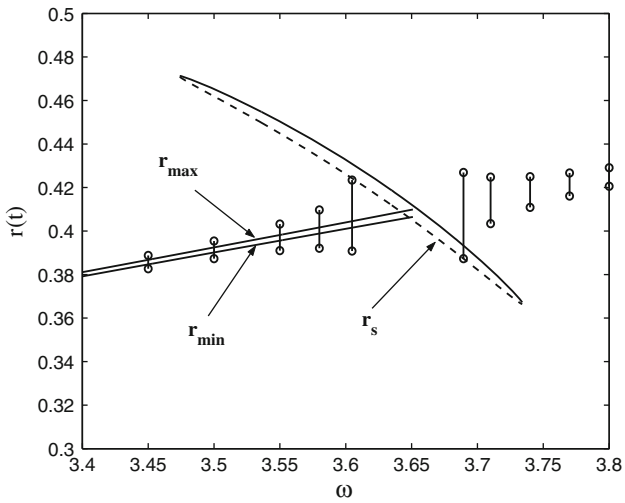

Fig. 7 Amplitude-frequency response and the modulation amplitude of slow flow limit cycle. Numerical simulation: *double circles*, analytical approximation: double lines on the left between *circles*; r_s: amplitude of saddles. Values of parameters are fixed as in Fig. 5

$$u_1(T_0,T_1,T_2) = \frac{R^3(T_1,T_2)}{4S}(H_1\cos(3ST_0+3\varphi(T_1,T_2)) - H_2\sin(3ST_0+3\varphi(T_1,T_2)))$$
$$v_1(T_0,T_1,T_2) = \frac{R^3(T_1,T_2)}{4S}(H_1\sin(3ST_0+3\varphi(T_1,T_2)) + H_2\cos(3ST_0+3\varphi(T_1,T_2))) \quad (44)$$

Substituting (43) and (44) into (42) and removing secular terms gives the following partial differential system on R and φ :

$$D_2R = 0,$$
$$D_2\varphi = -\frac{3R^4}{4S}(H_1^2+H_2^2) \quad (45)$$

Hence, the second-order approximate periodic solution of the slow flow (11) is given by

$$u(t) = R\cos vt + \frac{R^3}{4S}(H_1\cos(3vt) - H_2\sin(3vt))$$
$$v(t) = -R\sin vt + \frac{R^3}{4S}(H_1\sin(3vt) + H_2\cos(3vt)) \quad (46)$$

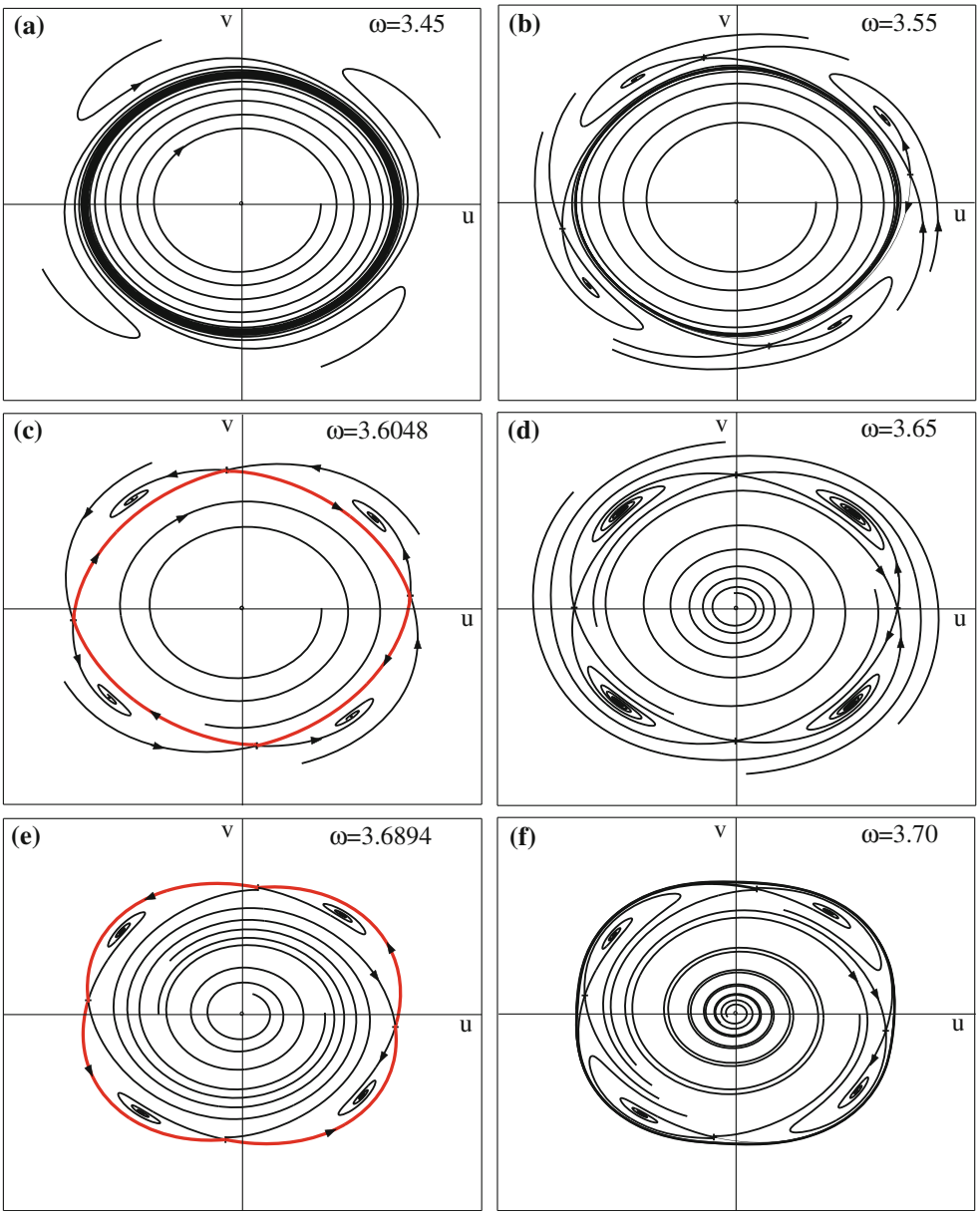

Fig. 8 Examples of phase portraits of the slow flow at different frequencies picked from Fig. 7. Values of parameters are fixed as in Fig. 6

where the amplitude R and the frequency v are now given, respectively, by

$$R = \sqrt{\frac{A}{B}} \tag{47}$$

$$v = S - \left(C + \frac{3R^2}{4S}\left(H_1^2 + H_2^2\right)\right)R^2 \tag{48}$$

Using (46), the modulated amplitude of quasiperiodic solutions is approximated by

$$r(t) = \sqrt{R^2 + \frac{R^6}{16S^2}\left(H_1^2 + H_2^2\right) + \frac{2R^4}{4S}\left(H_1\cos(4vt) - H_2\sin(4vt)\right)} \tag{49}$$

and the envelope of this modulated amplitude is delimited by r_{min} and r_{max} given by

$$r_{min} = \sqrt{R^2 + \frac{R^6}{16S^2}\left(H_1^2 + H_2^2\right) - \frac{2R^4}{4S}\sqrt{H_1^2 + H_2^2}} \tag{50}$$

$$r_{max} = \sqrt{R^2 + \frac{R^6}{16S^2}\left(H_1^2 + H_2^2\right) + \frac{2R^4}{4S}\sqrt{H_1^2 + H_2^2}} \tag{51}$$

Figure 7 depicts, in addition to the amplitude-frequency response, the modulated amplitudes of the slow flow limit cycle r_{min} and r_{max} as given by Eqs. (50) and (51). The comparaison between these analytical predictions (solid lines) and the numerical simulations (double circles) reveals that our analytical approach captures the modulation amplitude of the limit cycle close to the frequency-locking domain.

Figure 8 illustrates examples of phase portraits of the slow flow (37) for some values of ω picked from Fig. 7. For small values of ω, a slow flow limit cycle born by Hopf bifurcation exists and attracts all initial conditions. The related phase portrait is shown in subfigure (a) for $\omega = 3.45$. The subfigure (b) for $\omega = 3.55$ indicates the coexistence of two stable states, a stable periodic orbit and quasiperiodic response. As the forcing frequency varies, the stable limit cycle approaches the saddles and synchronizes as shown in subfigure (c) for the value $\omega = 3.6048$. Here the response of the system follows the 4:1 subharmonic frequency (see subfigure (d) for $\omega = 3.65$).

4 Conclusion

In this work, we have investigated the frequency-locking area in self-excited nonlinear oscillators subjected to harmonic excitation near the 3:1 and 4:1 subharmonic resonances. Analytical method based on a double averaging procedure is performed to approximate the quasiperiodic modulation domain and the frequency-locking area in the vicinity of the two resonances. We have focused our attention on the frequency-locking threshold in the case where the limit cycle disappears leaving the cycles outside the connection (see Figs. 4c, 8c). This corresponds to the left thresholds of the frequency-locking occurrence (see solid lines in Figs. 3, 7). It was shown that even though the synchronization domain near these secondary resonances is very small, the analytical treatment proposed here is efficient to capture the left threshold in which frequency-locking occurs.

To capture the right frequency-locking threshold in the case when the limit cycle disappears leaving the cycles inside the connection (see Figs. 4e, 8f), more efforts are required in term of approximating the quasiperiodic modulation domain.

References

1. Nayfeh AH, Younis MI, Abdel-Rahman EM (2007) Dynamic pull-in phenomenon in MEMS resonators. Nonlinear Dyn 48:153–163
2. Belhaq M, Fahsi A (2008) 2:1 and 1:1 frequency-locking in fast excited van der Pol–Mathieu–Duffing oscillator. Nonlinear Dyn 53(1–2):139–152
3. Fahsi A, Belhaq M, Lakrad F (2009) Suppression of hysteresis in a forced van der Pol–Duffing oscillator. Commun Nonlinear Sci Numer Simul 14(4):1609–1616
4. Bogoliubov NN, Mitropolsky YA (1961) Asymptotic methods in the theory of oscillations. Hindustan Publishing Company, Delhi
5. Nayfeh AH, Mook DT (1979) Nonlinear oscillations. Wiley, New York
6. Fahsi A, Belhaq M (2009) Hysteresis suppression and synchronization near 3:1 subharmonic resonance. Chaos Solitons Fractals 42:1031–1036
7. Belhaq M, Fahsi A (2009) Hysteresis suppression for primary and subharmonic 3:1 resonances using fast excitation. Nonlinear Dyn 57:275–286
8. Belhaq M, Houssni M (1999) Quasi-periodic oscillations, chaos and suppression of chaos in a nonlinear oscillator driven by parametric and external excitations. Nonlinear Dyn 18:1–24
9. Belhaq M, Guennoun K, Houssni M (2000) Asymptotic solutions for a damped non-linear quasi-periodic Mathieu equation. Int J Non-linear Mech 37:445–460
10. Rand RH, Guennoun K, Belhaq M (2003) 2:2:1 Resonance in the quasi-periodic Mathieu equation. Nonlinear Dyn 31:187–193
11. Rand RH, Morrison T (2005) 2:1:1 resonance in the quasi-periodic Mathieu equation. Nonlinear Dyn 40:195–203
12. Sah SM, Recktenwald G, Rand RH, Belhaq M (2008) Autoparametric quasiperiodic excitation. Int J Non-linear Mech 43:320–327
13. Krauskopf B (1995) On the 1:4 resonance problem. Dissertation, University of Groningen
14. Takens R (2001) Global analysis of dynamical systems: Festschrift dedicated to Floris Takens for his 60th birthday. In: Broer HW, Krauskopf B, Vegter G (ed) Taylor and Francis
15. Belhaq M, Fahsi A (1997) Higher-order approximation of subharmonics close to strong resonances in the forced oscillators. Comput Math Appl 33(8):133–144